Simultaneous optimization of confinement and thermal performance for heteroepitaxial InP on SoI hybrid lasers

Chengxin Pang, Henri Benisty, Mondher Besbes

Simultaneous optimization of confinement and thermal performance for heteroepitaxial InP on SoI hybrid lasers

C. Pang[a], H. Benisty*[a], M. Besbes[a]

[a]Laboratoire Charles Fabry, Institut d'Optique Graduate School, CNRS, Univ P Sud, 2 Avenue Augustin Fresnel, F-91127, Palaiseau, France

henri.benisty@institutoptique.fr

ABSTRACT

In new designs permitted by heteroepitaxial bonding of III-V active slabs onto nano-patterened SoI wafers, two constraints arise in the design: optical confinement and thermal performance. One require less silicon for the former and more silicon for the latter. We propose a mitigation strategy based on electromagnetism and a flip-flop algorithm.

Keywords: Waveguide, hybrid silicon laser, nanostructure

1. INTRODUCTION

The road to highly integrated photonic integrated circuits (PICs) can advantageously combine highly developed silicon technologies (notably based on SOI : silicon-on-insulator) fitted to large-scale integration with bonded InP-based wafers that provide active functions such as amplifiers and lasers. The present way to perform this bonding, pioneered by the team of Bowers at UCSD and by IBM/Intel work, privileges a sizable silicon dioxide spacer planarizing the silicon waveguide structure prior to bonding[1-5]. This strategy or polymer ones[6,7] does not optimize the thermal performance since a heat barrier is caused by the poor SiO_2 conductance. Following investigations that recently began on direct bonding without intermediate layer between InP and silicon[8,9], we discuss which possible patterned silicon waveguides can be implemented to get a good compromise between guiding properties and thermal properties. Grossly speaking, the former require tight optical confinement, thus maximizing the etched silicon (air) content. As for the thermal conductance, it relies best on silicon, and thus calls for the largest possible amount of silicon beneath the InP, as much as possible with topological in-plane continuity. We tackle these issues with a mode-solver and a variant of the "flip-flop" optimization[10] to decide where it is best to etch the silicon. We first describe the structures and the quantity we model in this section. In Sec. 2 we look at the way the nanostructures can act as "intermediate index materials", in the framework of the Effective Material Theory[11,12] for structured dielectrics in 1D or in 2D. In the third section, we present results of an optimization using the flip-flop algorithm[13] to decide on the best way such nanostructures can be arranged.

1.1 Directly bonded heteroepitaxial InP-SoI lasers.

In most schemes for integration of hybrid lasers, thermal management demands are a difficult issue. Heat is of course mainly generated by current injected in a multi-quantum-well active stack, with various Joule heating for access to this active area. Due to the poorer InP thermal conductance it does not evacuate very well through the InP side. In nearly all reported designs based on SOI, there is also an important heat barrier on this SOI side due to the systematic use of a thin isolating layer such as silica[1-5] or BCB (Benzo-cyclo-butene) polymer[6,7] inserted to ensure a reproducible bonding between the SOI and the flipped InP wafer piece.

An interesting variant leading to novel designs can be thought by making use of directly bonded silicon/InP systems. Wafer fusion between silicon and III-Vs has been known for about two decades, but InP/silicon interfaces have not been much studied, except for avalanche photodiodes in the late 90s, with the hope to get the best of both materials. Recently, some studies revived these attempts, in order to propose a new generation of InP/silicon lasers. The general idea is to make a large scale technology on silicon, and to cause adhesion of the InP wafer in such a way that only medium size areas (say a fraction of cm^2) are bonded at adequate places. This may require a first step of "expanding" an InP wafer into large dies stuck on a carrier or other alternatives. Practical studies in the lab still involve small pieces of silicon and InP, thereefore scaling up the whole process. In the following, we describe the structure more in detail.

1.2 Description of the structure

A cross-section of a typical structure investigated, based on 500 nm thick SOI[14], is presented in Fig.1a. In this structure, it is assumed that after bonding of the InP wafer, the InP wafer handle was removed thanks to a sacrificial layer, leaving a thick (~2 μm) buffer layer above the active region (MQW : multiple quantum well), where guiding is favored by the higher index of the MQW stack, as is classical. This thick layer is further shaper as a rather broad mesa, with no sizable confining influence on the guided mode properties. Confinement is enforced in the silicon wafer, but not through a single rectangular waveguide, as has usually been proposed until now, but rather as a structure system where the cladding of the central silicon core of width w_{Si} relies on a 1D nanostructure medium.

Such a nanostructured medium can be made of 1D thin grooves, or of 2D array of holes.[10] In these different cases, the equivalent EMT material is not the same, and the thermal properties are not the same either. We will work mostly in the sub-wavelength regime: when periodicity is involved along the guide axis especially, we will choose the period in such a way that no distributed feedback can take place around the operation wavelength, λ=1550 nm. Due to fabrication constraints, it is favorable to attempt the largest possible structures that are in this regime. This means in practice that distributed-feedback (DFB) effects of the well-known DFB laser or DBR types could take place at wavelength not much shorter, say 1300 nm.

As for the thermal performance, we want to get silicon "thermal bridges" between the upper InP part and the unpatterned silicon part of the SOI structure as close as possible to the center of the structure. To make this quantitative, based on thermal maps form known modeling works of such hybrid lasers, we use a thermal figure of merit that has the shape of Fig.1.b, a decreasing function with convex low-order polynomial behavior being sufficient to get an idea of what our generic idea of a thermal/optical mitigation procedure can provide; without the workload of a genuine coupled/optical model, as it seems too early to provide detailed data along this avenue.

2. DISCUSSION OF NANOSTRUCTURED CLADDING

2.1 One-dimensional (1D) nanostructured cladding

If we consider for instance 1D nanostructured media (Fig.1c,d) two options A and B can arise as regards the direction of the grooves.[10] In option A, the grooves are perpendicular to the waveguide axis, whereas in option B, they are in the same direction.

If one assume simply a periodic nanostructured medium of period a, it is tempting to model it with the tools of EMT, and to replace it by the corresponding anisotropic index of refraction. Polarization plays of course a big role.

What we will call a quasi TE mode, and is most often desired for common MQW stacks, is a mode whose electric field **E** lies mainly along the x axis of the wafer. Conversely a TM mode would have its main component of the electric field **E** along the y axis, and its magnetic field **H** along the y axis.

As a good approximation, even though channel waveguide modes have six nonzero components, we can replace a periodic cladding by an EMT. At such a stage, either a FE (finite element) mode solver with anisotropic indices is used – and quasi-TE and quasi-TM modes are retrieved in one overall run–, or a solver for isotropic indices is used, and the proper index of the EMT is used in conjunction with the proper mode hunt as follows:

For A-type grooves, and quasi-TE modes, **E** is rather along the interface, therefore the ordinary index of EMT theory should be used, that is the one corresponding to the average of the dielectric constant in the limit of a vanishing a/λ ratio. Denoting f the air-filling factor, we use the index n such that $n^2=f\times1+(1-f)\times\varepsilon_{Si}$. For quasi-TM modes, the same index would still hold, as the field **E** is still mainly along the interface.

For B-type grooves, and quasi-TE modes, **E** is now across the interfaces along x, therefore we have to use the extraordinary index, or in other words, the average of the inverse of the dielectric constant should be used in the same a/λ <<1 limit : $n^2=(f\times1^{-1}+(1-f)\times\varepsilon_{Si}^{-1})^{-1}$.

This B-type extraordinary index is generally quite smaller than the previous one. This means that for a given amount of air, more confinement of the guided wave shall be obtained. As we want to minimize the air content to reduce thermal barriers but still keep good guidance, we see that this second option is highly favored in the comparison.

2.2 Two-dimensional nanostructured cladding

A different option (Fig.1e) is a two-dimensional nanostructure: we can use an array of holes in the silicon to form the cladding. There are several good aspects in this choice: To make small air-filling factor, notably, requires very thin grooves, whose large aspect ratio can become prohibitive with respect to reasonable fabrication methods. Small air-filling factor in 2D can be achieved with much larger feature sizes. Typically, for round holes and triangular lattice, diameter to period ratio of the order of 0.25 are sufficient to get well below the air-filling factor f=0.1. If we remain in the frame of the EMT theory, we can guess that the effective index of such a cladding for TE mode will be intermediate between those of A and B structures of the same air-filling factor, given the span of local field geometries either normal or parallel to the local holes interfaces.

Thus, we cannot get as good a confinement as in the case of B-type structure for the *same* air-filling factor, but it is likely that we can fabricate much smaller air-filling factors in this strategy, hence a better compromise.

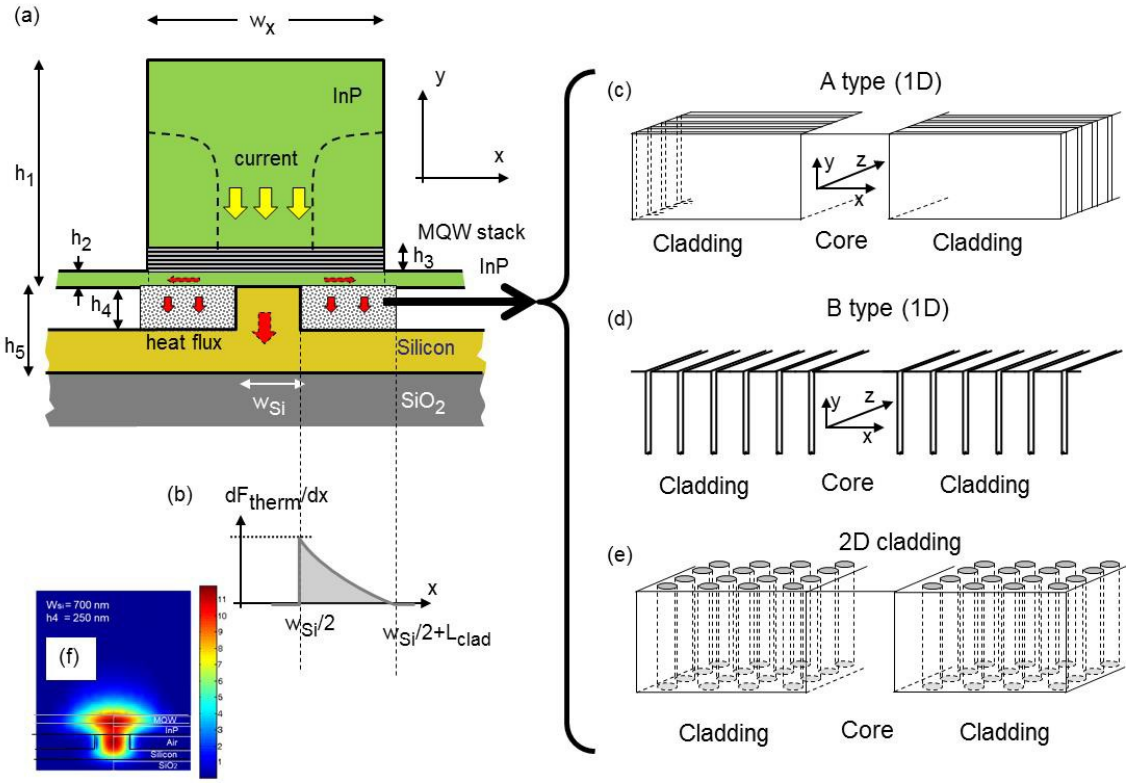

Figure 1. (a) general sketch of the hybrid laser structures, the detail of the grey cladding area is given in (c-e) ; (b) sketch of the profile of the thermal figure of merit attributed to the presence of silicon in the thermally interesting area; (c-e) various types of cladding : (c) type A, 1D; (d) type B, 1D ; (e) 2D cladding made of holes; (f) color map of the E_x field component in the case of an air cladding, with superimposed structure shown, for h_4=250 nm and w_{Si}=700 nm.

3. NUMERICAL RESULTS

3.1 Simulation method

In the simulation, we use a finite-element code and isotropic indices for simplicity. We pick-up only those modes whose main field corresponds to the chosen index. This technique still renders the main trends about the degree of confinement. For the 2D cladding case, we assume that the period will be relatively large to fully exploit the easier fabrication, therefore we use a 2D plane wave expansion[15,16] to get the actual effective index of a square lattice of perforated silicon as a function of the ratio a/λ and of the air-filling factor f (Fig.2)

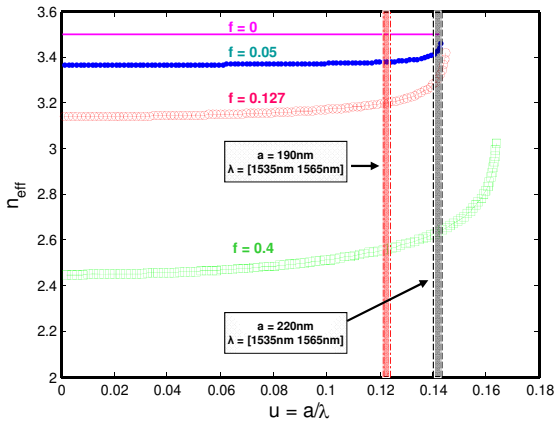

Figure 2. Effective refractive index of a square array of round holes in silicon as a function of ratio a/λ. The electric field is normal to the hole axis. The range associated to telecom C band (1535-1565 nm) is signaled for two periods : a=190 nm and a =220 nm. The correction is important at this period as we approach the photonic band gap.

3.2 Calculation results for the modes with various nanostructured cladding

Comparison of the different cladding solutions can be made by plotting important quantities of the calculated guided modes : the confinement factors of the mode in the MQW and in silicon, and of course their effective index. This is done in Fig. 3 for the various 1D A-type, 1D B-type and 2D cases indicated.

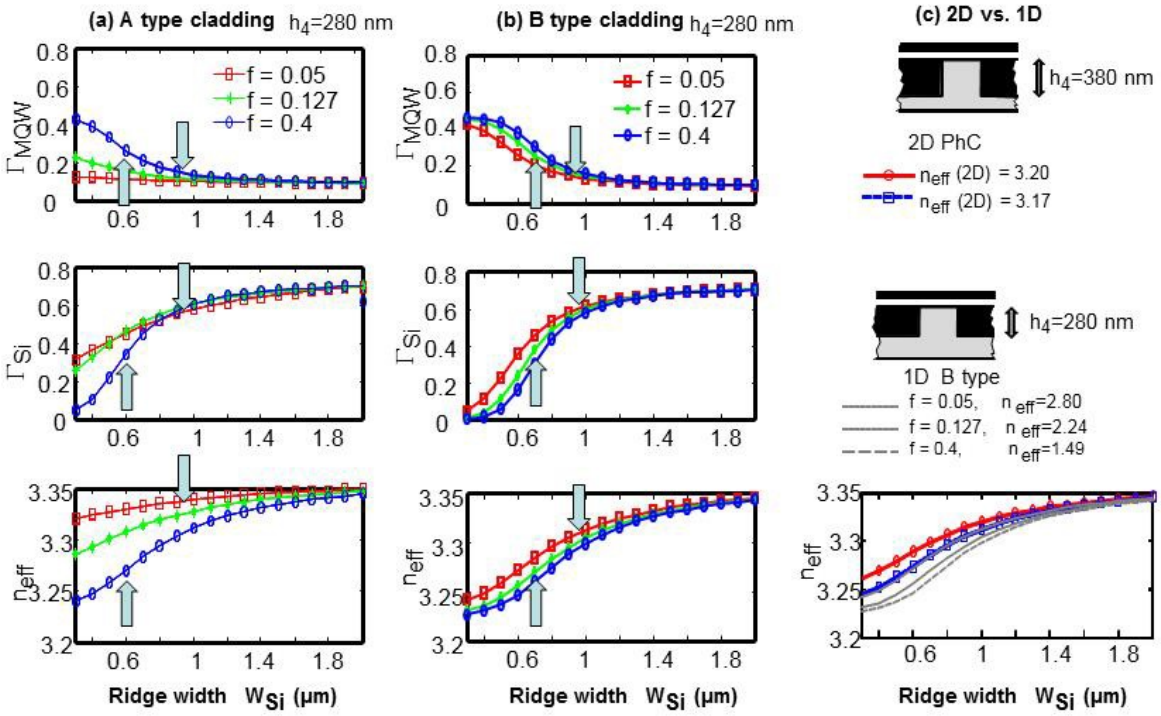

Figure 3. TE modes characteristics vs. silicon ridge width w_{Si} (a) results of MQW confinement factor, Si confinement factor and effective indices for A type cladding; (b) same for B type cladding; (c) comparison of 2D with a deeper etch (f=0.127) and 1D with a shallower etch.

By browsing through these calculations, by comparing for instance in Fig.3(a,b) the upward and downward arrows in the various graphs, it is seen that the higher effective indices of the A type cladding translate into poorer confinement in the

MQW than for the B-type one, which gives good results a large range of ridge width, allowing thus a design with more freedom. Fig.3c reports a calculation with a deeper etch that could be more easily reached with the hole arrays indicated in Fig.2, targeting large enough periods and thus "large" diameters on the order of 80 nm or so, for an air filling factor of f=0.127. With these parameters, it can attain the same kind of confinement as the B-type cladding reported as grey curves with a smaller air filling factor (f=*0.05*) and smaller etch depth (deeper would not be much feasible). Thus the 2D array seems to relax fabrication constraints sufficiently to allow guidance similar to the "good" one of the 1D variants, i.e. the B-type one which combines good confinement with low air-filling factor, and therefore good thermal conduction.

3.3 Flip-flop optimization

It may be tempting to consider more freedom in design than just an effective index cladding, be it of 1D or 2D nature. It is in principle possible to make grooves that are oriented along the waveguide axis, as for the B-type, but with any width and groove size, so that one could finely look for an optimum combination of good thermal properties, demanding more silicon, and good MQW confinement, demanding more air in the cladding. We thus digitized the cladding as a series of N "slices" allowing each to be made either of air or of silicon, and letting a flip-flop algorithm[10,13] evolve so as to choose at each slice the best option. We used an overall figure of merit[10] combining the MQW confinement factor Γ_{MQW} and the thermal figure of merit evoked in Fig.1b, that gives more weight to silicon close to the heat source according to an ad hoc but realistic polynomial decaying law for an interval of about 2 µm, symmetrically of course on each side of the silicon central ridge. To shorten the calculation, the more critical central slices were thinner than the outermost ones, but the largest were still small enough (~>100 nm) to affect the lateral evanescence of the mode not too much when switching materials from Si to air for instance in the flip-flop process. A pictorial view of the process and results is given in Fig.4.

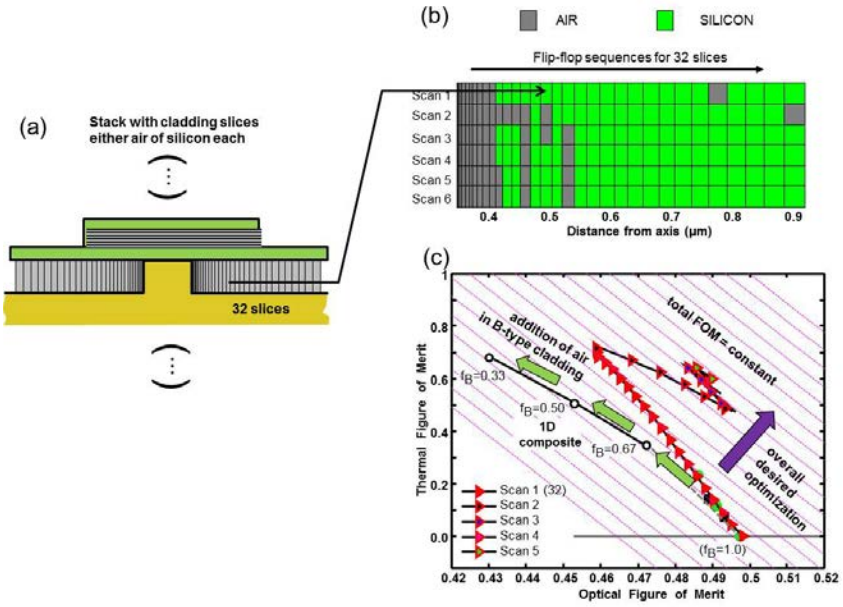

Figure 4. (a) sketch of where the slides lies to perform the flip-flop optimization, each slice being either air or silicon; (b) sequence obtained when optimizing along the direction of the arrow, with 5 successive scans; (c) Trajectory of the two optical and thermal figure of merits that make up the total figure of merit (triangles and black line) compared to the B-type cladding results using the same slices (hence no valid access to very small air filling factor f), showing the decrease of the optical figure of merit when too much silicon is added, starting from air (f=1 at the bottom).

Starting from an air-cladding (f=1), silicon is added first at the slices that are about 100 nm off the central ridge boundary (abscissa 400 nm off the center of the whole structure) , and almost no air is further introduced. Upon further scans, a more alternate pattern of air and silicon emerged between 400 and 600 nm abscissae, tending toward an effective material with about 25% air. A very fine mesh would be needed on the physics side. But on the contrary, from the fabrication point of view, the smallest group of air slices obtained have to be compatible with fabrication, (here we would target ~20 nm air slices, for which the required depth, say h_4= 250 nm is still at the boundary of feasibility).

3.4 Conclusion

There are several ways to exploit the novel possibility of directly bonded silicon-InP wafers for semiconductor lasers. We have shown that a B-type cladding, grooves parallel to the guide axis, is intrinsically better for optical confinement at a given thermal load. 2D cladding are probably the best compromise for feasible structures. Cleverly designed sequences can still be devised by application of the popular flip-flop algorithm, and the present approach could be revisited with a more accurate figure of merit than the partly arbitrary one we have selected in our example, using a FE thermal model.

3.5 Acknowledgements

The authors thank A. Talneau for useful discussions. This work was done under the French project COHEDIO of the P2N program of Agence Nationale de la Recherche (ANR).

REFERENCES

[1] Fang, A. W., Park, H., Jones, R., Cohen, O., Paniccia, M. J., Bowers, J. E., "A Continuous-Wave Hybrid AlGaInAs–Silicon Evanescent Laser," IEEE Phot. Technol. Lett. *18*, 1143-1145 (2006).

[2] Liang, D., Roelkens, G., Baets, R. and Bowers, J. E., "Hybrid Integrated Platforms for Silicon Photonics," *Materials*, *3*, 1782-1802 (2010).

[3] Park, H., Fang, A. W., Jones, R., Cohen, O., Raday, O., Sysak, M. N., Paniccia, M. J. andBowers, J. E., "A hybrid AlGaInAs-silicon evanescent waveguide photodetector," *Opt. Express 15*, 6044-6052 (2007).

[4] Kuo, Y.-H., Chen H-W.,, Bowers J.E., "High speed hybrid silicon evanescent electro absorption modulator," *Opt. Express, 16*, 9936-9941 (2008).

[5] Sun, X., Zadok, A., Shearn, M. J., Diest, K. A., Ghaffari, A., Atwater, H.A., Scherer, A. and Yariv, A., "Electrically pumped hybrid evanescent Si/InGaAsP lasers,"*Opt. Lett. 34,* 1345-1347 (2009).

[6] Stankovic, S., Roelkens, G., Van Thourhout, D., Jones, R., Sysak, M., Heck, J., "1310nm evanescent hybrid III-V/Si laser based on DVS-BCB bonding," Integrated Photonics Research, Silicon and Nano-Photonics (IPR), IWC3, Canada, Toronto, 28-30 June (2011).

[7] Stankovic, S., Roelkens, G., Van Thourhout, D., Baets, R., Jones, R., Sysak M., and Koch, B., "Hybrid III-V/Silicon laser based on DVS-BCB bonding," in Proc. 13th Ann. Symp. IEEE/LEOS Benelux Chapter, Enschede, Netherlands, p.139-142 (2008).

[8] Ilovitsh, T., Bakis, I., Shubely, M., Shekel, E., Ben-Ezra, Y., Sukenik, C. N., Zadok, A., "Wafer bonding techniques for hybrid silicon photonic devices based on surface modifications," 14th International Conference on Transparent Optical Networks (ICTON), Coventry, 2-5 July (2012).

[9] Talneau, A., Chouteau, D., Mauguin, O., Largeau, L., Sagnes I., and Patriarche, G., "Heteroepitaxial bonding of GaInAs quantum wells on Si: A new approach towards photonic integration on Si for devices operating at 1.55µm," 24th Int. Conf. on Indium Phosphide and Related Materials, paper Tu-2E.2, Santa Barbara, CA USA, August 27-30 (2012).

[10] Pang, C., Benisty, H., "Nanostructured silicon geometries for directly bonded hybrid III–V- silicon active devices," Photon Nanostruct: Fundam Appl (2013), http://dx.doi.org/10.1016/j.photonics.2012.12.003

[11] Lalanne, P., "Effective medium theory applied to photonic crystals composed of cubic or square cylinders," *Appl. Opt.* 27*,* 5369-5380 (1996).

[12] Bergman, D., "The dielectric constant of a composite material - a problem in classical physics," *Phys. Rep.* 43, 377-407 (1978).

[13] Southwell, W. H., "Coating design using very thin high- and low-index layers" *Appl. Opt. 24*, 457-460 (1985).

[14] Lamponi, M., Keyvaninia, S., Jany, C., Poingt, F., Lelarge, F., de Valicourt, G., Roelkens, G., Van Thourhout D., Messaoudene, S.,Fedeli, J.-M. and Duan, G.-H., "Low Threshold Heterogeneously Integrated InP/SOI Lasers with a Double Adiabatic Taper Coupler," *IEEE Phot. Technol. Lett.* 24, 76-78 (2012).

[15] David, A., Benisty H., and Weisbuch C., "Fast factorization rule and plane-wave expansion method for two-dimensional photonic crystals with arbitrary hole-shape," *Phys.Rev.B 73*, 075107 (2006).

[16] Plihal, M., and Maradudin, A. A., "Photonic band structure of two-dimensional systems : The triangular lattice," *Phys. Rev. B* 44, 8565 (1991).